Hydrobiologia (2019) 842:127–141
https://doi.org/10.1007/s10750-019-04031-0

PRIMARY RESEARCH PAPER

Combined effects of CO_2 level, light intensity, and nutrient availability on the coccolithophore *Emiliania huxleyi*

Yong Zhang · Feixue Fu · David A. Hutchins · Kunshan Gao

Received: 10 September 2018 / Revised: 9 July 2019 / Accepted: 20 July 2019 / Published online: 2 August 2019

Abstract Continuous accumulation of fossil CO_2 in the atmosphere and increasingly dissolved CO_2 in seawater leads to ocean acidification (OA), which is known to affect phytoplankton physiology directly and/or indirectly. Since increasing attention has been paid to the effects of OA under the influences of multiple drivers, in this study, we investigated effects of elevated CO_2 concentration under different levels of light and nutrients on growth rate, particulate organic (POC) and inorganic (PIC) carbon quotas of the coccolithophorid *Emiliania huxleyi*. We found that OA treatment (pH 7.84, CO_2 = 920 µatm) reduced the maximum growth rate at all levels of the nutrients tested, and exacerbated photo-inhibition of growth rate under reduced availability of phosphate (from 10.5 to 0.4 µmol l^{-1}). Low nutrient levels, especially lower nitrate concentration (8.8 µmol l^{-1} compared with 101 µmol l^{-1}), decreased maximum growth rates. Nevertheless, the reduced levels of nutrients increased the maximum PIC production rate. Decreased availability of nutrients influenced growth, POC and PIC quotas more than changes in CO_2 concentrations. Our results suggest that reduced nutrient availability due to reduced upward advective supply because of ocean warming may partially counteract the negative effects of OA on calcification of the coccolithophorid.

Keywords Calcification · CO_2 · Coccolithophore · Growth · Light · Nutrient

Introduction

Rising atmospheric CO_2 level leads to increasing seawater CO_2 concentration and decreasing pH, which is known as ocean acidification (OA) (Caldeira &

Handling editor: Judit Padisák

Electronic supplementary material The online version of this article (https://doi.org/10.1007/s10750-019-04031-0) contains supplementary material, which is available to authorized users.

Y. Zhang · K. Gao (✉)
State Key Laboratory of Marine Environmental Science & College of Ocean and Earth Sciences, Xiamen University, Xiamen 361005, People's Republic of China
e-mail: ksgao@xmu.edu.cn

K. Gao
Jiangsu Key Laboratory of Marine Bioresources and Environment, Jiangsu Ocean University, Lianyungang 222005, People's Republic of China

K. Gao
Laboratory for Marine Ecology and Environmental Science, Qingdao National Laboratory for Marine Science and Technology, Qingdao 266071, People's Republic of China

F. Fu · D. A. Hutchins
Department of Biological Sciences, University of Southern California, Los Angeles, CA 90089, USA

Wickett, 2003). On the other hand, accumulating atmospheric CO_2 also leads to global and ocean warming, which enhances water column stratification and reduces the thickness of the upper mixed layer (UML) in the open ocean (Wang et al., 2015). This increases light exposures to phytoplankton cells dwelling therein (Steinacher et al., 2010). In addition, enhanced stratification reduces upward transport of nutrients from the deep ocean to the UML (Behrenfeld et al., 2006), limiting the nutrient concentrations in this layer.

Coccolithophores take up CO_2 and/or HCO_3^- from seawater for photosynthetic carbon fixation, and use HCO_3^- for calcification. Calcification processes generate CO_2 due to production of protons, influencing CO_2 influx into the oceans (Rost & Riebesell, 2004). Growth rate, particulate organic (POC) and inorganic carbon (PIC) production rates of *Emiliania huxleyi* (Lohmann) W. W. Hay & H. P. Mohler, the most abundant calcifying coccolithophore species, display optimum responses to a broad range of CO_2 levels (Bach et al., 2011; Zhang et al., 2018). Growth, POC and PIC production rates could increase, decrease, or be unaffected by rising CO_2 concentrations based on climate change scenarios (400–1000 µatm) (Langer et al., 2009; Richier et al., 2011; Bach et al., 2015; Jin et al., 2017). Differences in sampling locations, experimental setups, deviations in the measuring methods, and intraspecific differences can generally be responsible for the differential responses of growth, POC and PIC productions to rising CO_2 in *E. huxleyi* (Langer et al., 2009; Meyer & Riebesell, 2015; Hutchins & Fu, 2017).

Coccolithophore POC production as well as growth rates usually increase with increased light intensity, level off at saturated light intensity and decline at inhibiting high light intensity (Zhang et al., 2015; Jin et al., 2017). Light availability modulates energy budgets in photosynthetic organisms, and algae have developed strategies to acclimate to changing light intensities (Geider et al., 1997; Gao et al., 2012a). At low light intensities, the ratio of light-harvesting protein to photosystem II (PSII) reaction center proteins is large, which allows *E. huxleyi* to absorb more energy. At high light intensity, the ratio of photo-protection proteins to PSII reaction center proteins is large, displaying photoacclimation strategies (McKew et al., 2013).

Nitrogen is required for the biosynthesis of proteins and other macromolecules, including chlorophyll (Riegman et al., 2000). Phosphorus is required for the synthesis of nucleic acids, ATP, and phospholipids in cell membranes (Shemi et al., 2016). Suboptimal nutrient concentrations usually reduce growth and photosynthetic carbon fixation rates (Cloern 1999; Kim et al., 2007; Harrison & Li, 2008). Nevertheless, low nutrient concentrations often enhance the PIC quotas of *E. huxleyi* because it can arrest cell cycling and lengthen the G1 phase where calcification occurs (Müller et al., 2008; McKew et al., 2015), and thus increases in PIC quotas are smaller at high CO_2 than at low CO_2 levels (Matthiessen et al., 2012; Rouco et al., 2013). In addition, rising CO_2 levels can decrease growth rates at high phosphate concentration, but did not affect growth rates at low phosphate concentration (Matthiessen et al., 2012). These studies imply that fitness-relevant traits of *E. huxleyi* may be altered in future high-CO_2 and low-nutrient oceans.

Changes in light or solar radiation are known to regulate growth, photosynthesis, calcification, and photoprotective strategies in coccolithophores (Feng et al., 2008; Gao et al., 2012b). At low light levels, coccolithophores tend to increase CO_2 uptake efficiency, while under non-limiting light levels such a mechanism disappears (Kottmeier et al., 2016). Under OA conditions, *Gephyrocapsa oceanica* decreased its growth rate, POC and PIC production rates within a wide range of light intensities (50–800 µmol photons m^{-2} s^{-1}) (Zhang et al., 2015). Feng et al. (2008) found that a Sargasso Sea isolate of *E. huxleyi* decreased PIC:POC ratios under OA only at elevated irradiances. Under fluctuating higher levels of natural solar radiation, however, OA treatment increased the growth and POC production rates of *E. huxleyi* (Jin et al., 2017). It appears that growth under different light environments could result in differential responses to rising CO_2 concentrations in growth and POC production of *E. huxleyi* and *G. oceanica*.

Recently, researchers have paid increasing attention to the effects of ocean acidification or warming under multiple stressors on marine phytoplankton (Brennan & Collins, 2015; Boyd et al., 2016; Hutchins & Fu, 2017; Boyd et al., 2018). In addition, physiological responses of phytoplankton to one environmental factor may be synergistically, antagonistically, or neutrally affected by others (Tong et al., 2016; Müller et al., 2017). Optimal CO_2 levels and maximal values for growth rate, photosynthetic carbon fixation, and calcification rates are modulated by temperature

and light intensity (Feng et al. 2008, Sett et al., 2014; Zhang et al., 2015).

Under chemostat cultures, rising CO_2 levels were found to increase the POC quotas of a non-calcifying strain of *E. huxleyi* (PML 92A) and a calcifying strain of *E. huxleyi* (PML B92/11) at low nutrient concentration and high light intensity (Leonardos & Geider, 2005; Borchard et al., 2011). However, relatively few studies have observed the combined effects of nutrients, CO_2, and light intensity on physiological performances of coccolithophores (Feng et al., 2017; Boyd et al., 2018). To investigate responses of *E. huxleyi* to multiple environmental drivers, we employed dilute batch cultures, and investigated growth rates and POC and PIC quotas at different levels of CO_2, light, dissolved inorganic nitrogen (DIN) and phosphate concentrations (DIP).

Materials and methods

Experimental design

Emiliania huxleyi strain PML B92/11, one of the most commonly studied strains of *E. huxleyi*, was isolated from Norwegian coastal waters and obtained from the culture collection at Plymouth Marine Laboratory. Nitrate and phosphate concentrations, daily irradiances, and CO_2 levels in Norwegian coastal waters under present-day conditions and projected conditions for 2100 are shown in Table S1 (Larsen et al., 2004; Omar et al., 2010; Boyd et al., 2015). The alga was cultured in dilute batch cultures in Aquil medium (final cell concentrations were 20,000 to 170,000 cells ml^{-1}) at 20°C in a light chamber (GXZ, Dongnan Instrument Company) under a 12:12-h light:dark cycle (light period: 8:00 a.m. to 8:00 p.m.). The Aquil medium was prepared according to Sunda et al. (2005) with the addition of 2200 µmol l^{-1} bicarbonate, resulting in initial total alkalinity (TA) of 2200 µmol l^{-1}, close to that of surface seawater in the South China Seas (Chou et al., 2005). Initial dissolved inorganic nitrogen (DIN) and phosphate (DIP) concentrations in Aquil were 100 µmol l^{-1} and 10 µmol l^{-1}, respectively (HNHP). For Aquil medium with low DIN concentration (LN) and low DIP concentration (LP), the nitrate and phosphate concentrations were reduced to 8 µmol l^{-1} and 0.4 µmol l^{-1}, respectively (Table S2). The experiment was performed in three parts. The first part (Part I) was conducted at HNHP treatment, the second one (Part II) was at LN treatment, and the third one (Part III) was at LP treatment (Fig. S1).

First, we grew the algae in high nitrate and high phosphate concentrations (HNHP, Part I) at 80 ± 5 µmol photons m^{-2} s^{-1} of photosynthetically active radiation (PAR) for 8 generations (6 days, acclimation culture) (Fig. S1). Then, the cells were grown under the same conditions for another 8 generations (6 days, experimental culture). On the 6th day, we took samples and measured growth rates and POC and PIC quotas. Then, the HNHP-grown cells were transferred to 120 ± 8 µmol photons m^{-2} s^{-1}, and were acclimated for 8 generations followed by another 8 generations for experimental sampling, respectively. Samples were taken as above for measurements of growth rate, POC and PIC quotas. After that, the cells were transferred stepwise to 200 ± 17 µmol photons m^{-2} s^{-1}, then to 320 ± 16 µmol photons m^{-2} s^{-1}, and to 480 ± 30 µmol photons m^{-2} s^{-1}, and acclimated for 8 generations followed by experimental culturing for 4 days under each light intensity. On the 4th day, growth rates and POC and PIC quotas were measured. Light intensities were measured using a PAR sensor (PMA 2132, Solar Light Company, Glenside). Second, we incubated the cells in low nitrate and high phosphate concentrations (LN, Part II), and transferred them from low to high light intensities in the same way as described above. Third, we incubated the algae in high nitrate and low phosphate concentrations (LP, Part III), and transferred them from low to high light intensities, and measured growth rate, POC and PIC quotas on the 4th, 5th or 6th days.

Under each nutrient treatment, the Aquil medium was aerated for 24 h at 20 °C (PVDF 0.22 µm pore size, Simplepure, Haining) with air containing 400 µatm or 1000 µatm pCO_2 (4 replicates at each CO_2 level). The dry air/CO_2 mixture was humidified with deionization water prior to the aeration to minimize evaporation. Then, the Aquil medium was filtered (0.22 µm pore size, Polycap 75 AS, Whatman) and carefully pumped into autoclaved 500-ml polycarbonate bottles (Nalgene). The bottles were filled with the culture medium with no headspace to minimize gas exchange after the cells were inoculated. Carbonate chemistry parameters (TA and pH) were measured at the beginning and end of the experiment.

For the dilute batch cultures, initial cell concentration was 200 cells ml^{-1} and cells were acclimated to the experimental treatments for at least 8 generations before starting the experiment (Table S3). Culture bottles were rotated twice at 10:00 a.m. and 6:00 p.m. To minimize changes in carbonate chemistry, final cell concentrations were lower than 170,000 cells ml^{-1}, and changes in dissolved inorganic carbon (DIC) concentrations were less than 10% (0.5–9.1%).

Nutrient concentrations, total alkalinity, and pH_T measurements

Samples for determination of inorganic nitrogen and phosphate concentrations were taken during the middle of light period using a syringe filter (0.22 μm pore size, Haining) and measured with a scanning spectrophotometer (Du 800, Beckman Coulter) according to Hansen & Koroleff (1999). The nitrate was reduced to nitrite by zinc cadmium reduction method before its concentration was determined.

Carbonate chemistry parameters were calculated from total alkalinity (TA), pH_T (total scale), phosphate, temperature, and salinity using the CO2SYS (Pierrot et al., 2006). In the final days of incubation, 25 mL samples for TA measurements were filtered (0.22 μm pore size, Syringe Filter) under moderate pressure of 200 mbar using a pump (GM-0.5A, JINTENG) and stored at 4 °C for a maximum of 7 days. TA was measured at 20 °C by potentiometric titration (AS-ALK1+, Apollo SciTech) according to Dickson et al. (2003). Samples for pH_T measurements were syringe-filtered (0.22 μm pore size), and the bottles were filled with overflow and closed immediately. The pH_T was immediately measured at 20 °C with a pH meter (Benchtop pH, Orion 8102BN) calibrated with an equimolar pH buffer (Tris HCl, Hanna) which is isosmotic with seawater (Dickson, 1993). Carbonic acid constants K_1 and K_2 were taken from Roy et al. (1993).

Cell density measurements

In the final days of the incubations (4th, 5th or 6th days), ~ 25 ml samples were taken from the incubation bottles at ~ 2:30 p.m. Cell concentrations and cell diameter (D) were measured using a Z2 Coulter Particle Count and Size Analyzer (Beckman Coulter). The diameter of detected particles was set to 3–7 μm in the instrument, which excluded any detached coccoliths (Müller et al., 2012). Cell concentrations were also measured by microscopy (ZEISS), and variation in measured cell concentration between two methods was ± 7.9% (Fig. S2). Average growth rate (μ) was calculated according to the equation: $\mu = (\ln N_1 - \ln N_0)/d$, where N_0 is 200 cells ml^{-1} and N_1 is the cell concentration in the final days of experiment, and d is the growth time span in days. *E. huxleyi* cells were spherical and its cell volume with coccoliths was calculated according to the equation: $V = 3.14 \times (4/3) \times (D/2)^3$ (Müller et al., 2012).

Particulate organic (POC) and inorganic carbon (PIC) quota measurements

GF/F filters, pre-combusted at 450°C for 8 h, were used to filter the samples of total particulate carbon (TPC) and particulate organic carbon (POC). TPC and POC samples were stored at − 20°C. For POC measurements, samples were fumed with HCl for 12 h to remove inorganic carbon, and samples for TPC measurements were not treated with HCl. All samples were dried at 60°C for 12 h, and analyzed using a Perkin Elmer Series II CHNS/O Analyzer 2400 instrument (Perkin Elmer Waltham, MA). Particulate inorganic carbon (PIC) quota was calculated as the difference between TPC quota and POC quota. POC and PIC production rates were calculated by multiplying cellular contents with μ (d^{-1}), respectively. Variations in measured carbon content between the four replicates were calculated to be 1–13% in this study.

Determination of growth rate at different dissolved inorganic phosphate (DIP) concentrations at LC

5 L Aquil media was enriched with 100 μmol l^{-1} DIN, aerated for 24 h at 20°C with air containing 400 μatm pCO_2, sterilized by filtration (0.22 μm pore size, Polycap 75 AS, Whatman), and then pumped into autoclaved 250 mL PC bottles. 10 μmol l^{-1}, 3 μmol l^{-1}, 1.5 μmol l^{-1}, 0.5 μmol l^{-1}, 0.25 μmol l^{-1} DIP (initial concentration) were, respectively, achieved by adding phosphate into Aquil media with three replicates at each DIP concentration. 200 cells ml^{-1} were inoculated into the Aquil media and all samples were first cultured at 200 μmol photons m^{-2} s^{-1} for 4 days. Then, 1 ml culture solution at 0.5–10 μmol l^{-1} DIP or 2.5 ml culture solution at 0.25 μmol l^{-1} DIP (initial cell concentrations were

200 cells ml^{-1} in all DIP concentrations) was inoculated into the Aquil media and cultured for another 4 days. Final cell concentration in the second incubation was measured using a Z2 Coulter Particle Count and Size Analyzer (Beckman Coulter).

Data analysis

Responses of growth rates, POC and PIC quotas or production rates, and PIC:POC ratio to incubation light intensities were fitted using the model provided by Eilers and Peeters (1988): $y = PAR/(A \times PAR^2 + B \times PAR + C)$, where the parameters A, B, and C are fitted in a least square manner. The apparent light use efficiency, the slope (*alpha*), for each light response curve was estimated as *alpha*= 1/C. The maximum values (V_{max}) of growth, POC and PIC production rates were calculated according to $V_{max} = 1/(B + 2\sqrt{A \times C})$.

A three-way ANOVA was used to determine the main effect of dissolved inorganic nitrogen or phosphate concentrations, CO_2, light intensity, and their interactions for these variables. A two-way ANOVA was performed to test the main effect of nitrate or phosphate concentrations, CO_2, and their interactions on fitted α and V_{max} of growth, POC and PIC production rates. When necessary, a Tukey Post hoc (Tukey HSD) test was used to identify the differences between two CO_2 levels, nitrate or phosphate concentrations, or light intensities. A Shapiro–Wilk's test was conducted to test residual normality and a Levene test was used to test for variance homogeneity of significant data. Statistical analysis was conducted by using R and the significance level was set at $P < 0.05$.

Results

Dissolved inorganic nitrogen and phosphate concentrations, and carbonate chemistry parameters

At the HNHP treatment, the dissolved inorganic nitrogen (DIN) and phosphate (DIP) concentrations, being 101 ± 1.1 μmol l^{-1} and 10.5 ± 0.2 μmol l^{-1}, respectively, at the beginning of the experiments, declined to 92.8 ± 1.6 μmol l^{-1} and 9.7 ± 0.2 μmol l^{-1}, respectively, at the end of incubations (Table S2). In the LN treatment, DIN concentrations were 8.8 ± 0.1 μmol l^{-1} at the beginning of the experiment and were 1.0 ± 0.4 μmol l^{-1} at the end of the experiment. In the LP treatment, DIP concentrations were 0.4 ± 0.1 μmol l^{-1} at the beginning of the experiment, and were below the detection limit (< 0.04 μmol l^{-1}) at the end of the experiment.

Under the low CO_2 (LC) treatment, pCO_2 levels of the seawater declined by 16% at HNHP, 19% at LN, and 8% at LP, and pH values increased by 0.07 at HNHP, 0.06 at LN, and 0.02 at LP treatments during the incubations, respectively (all $P < 0.05$) (Table 1). At the high CO_2 (HC) treatment, pCO_2 levels of the seawater declined by 23% at HNHP, 21% at LN, and 32% at LP, and pH values increased by 0.1 at HNHP, 0.09 at LN, and 0.15 at LP treatments during the incubations (all $P < 0.05$). Average pCO_2 levels were 410 μatm for all LC treatments, and were 920 μatm for all HC treatments.

Growth rate

Growth rates of *E. huxleyi* increased with elevated light intensity up to 200 μmol photons m^{-2} s^{-1} and significantly declined thereafter (all $P < 0.001$) (Fig. 1, Table 2). Compared to the LC treatment, growth rates at HC were 2%–7% lower at HNHP ($P < 0.05$), 5%–9% lower at LN ($P < 0.01$), and 3%–24% lower at LP ($P < 0.01$), respectively (Table S4). Under the LP treatment, HC-induced reduction of growth rate was greatest at 480 μmol photons m^{-2} s^{-1} (Fig. 1c).

At LC, growth rate at LN was similar to that at HNHP under 80 μmol photons m^{-2} s^{-1} ($P = 0.82$), and was significantly lower than at HNHP under optimal and supra-optimal light intensities ($P < 0.01$ for 200 μmol photons m^{-2} s^{-1}; $P = 0.005$ for 480 μmol photons m^{-2} s^{-1}). At HC, growth rates at LN were significantly lower than those at HNHP under limited, optimal, and supra-optimal light intensities ($P < 0.01$ for 80, 200, 480 μmol photons m^{-2} s^{-1}) (Fig. 1a, b).

At LC and 80 μmol photons m^{-2} s^{-1}, growth rate at LP was lower than at HNHP ($P < 0.001$); while at 120–480 μmol photons m^{-2} s^{-1}, growth rates were not significantly different between LP and HNHP treatments (all $P > 0.1$) (Fig. 1, Table S4). At HC and at 80, 120, and 480 μmol photons m^{-2} s^{-1}, growth rates were significantly lower at LP than at HNHP; at 200 and 320 μmol photons m^{-2} s^{-1}, growth rates were not significantly different between LP and HNHP treatments (both $P > 0.05$). At the low phosphate

Table 1 Carbonate chemistry parameters of the seawater at the beginning and end of the incubations at different nutrient conditions and pCO_2 levels

		pCO_2 (µatm)	pH (total scale)	TA (µmol l^{-1})	DIC (µmol l^{-1})	HCO_3^- (µmol l^{-1})	CO_3^{2-} (µmol l^{-1})	CO_2 (µmol l^{-1})	Ω calcite
HNHP									
LC	Before	510 ± 17^a	8.04 ± 0.01^a	2228 ± 17^a	2004 ± 20^a	1829 ± 21^a	159 ± 2^a	16 ± 1^a	3.8 ± 0.1^a
	End	428 ± 57^b	8.11 ± 0.05^b	2225 ± 24^a	1967 ± 22^b	1773 ± 34^b	180 ± 18^a	14 ± 2^b	4.3 ± 0.5^a
HC	Before	1210 ± 53^a	7.71 ± 0.02^a	2219 ± 19^a	2131 ± 22^a	2010 ± 22^a	81 ± 2^a	39 ± 2^a	1.9 ± 0.1^a
	End	935 ± 139^b	7.81 ± 0.06^b	2225 ± 24^a	2098 ± 12^b	1966 ± 17^b	102 ± 14^b	30 ± 4^b	2.4 ± 0.3^b
LN									
LC	Before	483 ± 23^a	8.06 ± 0.02^a	2204 ± 10^a	1973 ± 10^a	1796 ± 13^a	162 ± 6^a	16 ± 1^a	3.9 ± 0.1^a
	End	391 ± 39^b	8.12 ± 0.03^b	2123 ± 38^b	1866 ± 45^b	1679 ± 48^b	175 ± 9^b	13 ± 1^b	4.2 ± 0.2^b
HC	Before	1126 ± 66^a	7.73 ± 0.02^a	2201 ± 3^a	2105 ± 7^a	1983 ± 9^a	85 ± 4^a	36 ± 2^a	2.02 ± 0.1^a
	End	888 ± 114^b	7.82 ± 0.05^b	2142 ± 38^b	2016 ± 47^b	1890 ± 49^b	98 ± 8^b	29 ± 4^b	2.4 ± 0.2^b
LP									
LC	Before	397 ± 16^a	8.14 ± 0.02^a	2248 ± 30^a	1982 ± 22^a	1777 ± 17^a	192 ± 8^a	13 ± 1^a	4.6 ± 0.2^a
	End	365 ± 24^b	8.16 ± 0.02^a	2219 ± 20^b	1942 ± 22^b	1731 ± 25^b	199 ± 8^a	12 ± 1^b	4.8 ± 0.2^a
HC	Before	1140 ± 110^a	7.73 ± 0.04^a	2215 ± 41^a	2128 ± 46^a	2005 ± 46^a	86 ± 7^a	37 ± 4^a	2.1 ± 0.2^a
	End	780 ± 43^b	7.88 ± 0.02^b	2228 ± 14^a	2084 ± 11^b	1941 ± 12^b	117 ± 6^b	25 ± 1^b	2.8 ± 0.1^b

TA and pH samples were collected and measured before and in the final days of the experiment

Superscript letters (a and b) indicate statistical difference between the beginning and end of the incubations under low or high pCO_2 level (Tukey Post hoc, $P < 0.01$). The values are expressed as mean ± SD calculated from all light intensities

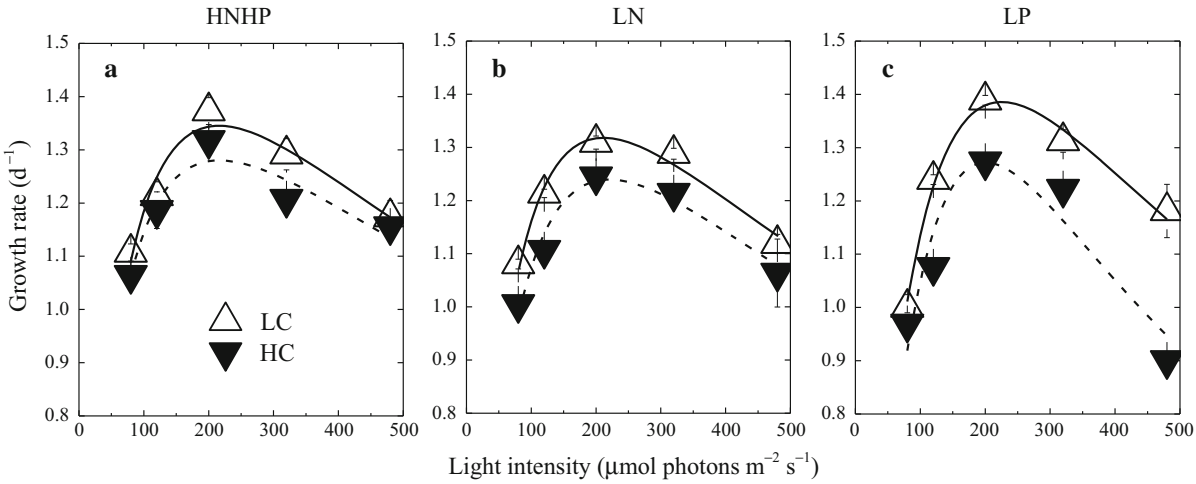

Fig. 1 Growth rate of *Emiliania huxleyi* as a function of light intensities at low pCO_2 (LC, hollow) and high pCO_2 levels (HC, solid) under **a** high dissolved inorganic nitrogen (DIN) and phosphate (DIP) concentrations (HNHP), **b** low DIN and high DIP concentrations (LN), and **c** high DIN and low DIP concentrations (LP). The lines in each panel were fitted using the model provided by Eilers and Peeters (1988). The values represent the mean ± standard deviation for four replicates

concentration, growth rate of *E. huxleyi* was more sensitive to changes in light intensity and CO_2 concentration.

POC quotas

In HNHP or LP treatments at LC, POC quotas were not significantly different at 80–200 µmol photons m^{-2}

Table 2 Results of three-way ANOVAs of the impacts of dissolved inorganic nitrogen or phosphate concentrations, pCO_2, light intensity, and their interaction on growth rate, POC and PIC quotas, and PIC:POC ratio

Factor	*F* value	*P* value	Factor	*F* value	*P* value
Growth rate (d^{-1})					
N	215.9	< 0.001	P	1015.5	< 0.001
C	547.8	< 0.001	C	213.3	< 0.001
L	1330.4	< 0.001	L	1863.8	< 0.001
N × C	9.1	= 0.004	P × C	147.6	< 0.001
N × L	11.8	< 0.001	P × L	274.4	< 0.001
C × L	18.3	< 0.001	C × L	11.1	< 0.001
N × C × L	4.1	= 0.006	P × C × L	19.7	< 0.001
POC quota (pg C $cell^{-1}$)					
N	27.1	< 0.001	P	13.7	< 0.001
C	0.6	= 0.435	C	0.1	= 0.731
L	34.7	< 0.001	L	103.2	< 0.001
N × C	13.2	< 0.001	P × C	14.5	< 0.001
N × L	17.9	< 0.001	P × L	0.4	= 0.780
C × L	1.0	= 0.432	C × L	21.6	< 0.001
N × C × L	1.9	= 0.125	P × C × L	7.3	< 0.001
PIC quota (pg C $cell^{-1}$)					
N	544.0	< 0.001	P	619.1	< 0.001
C	70.5	< 0.001	C	105.8	< 0.001
L	71.2	< 0.001	L	55.3	< 0.001
N × C	2.8	= 0.098	P × C	6.3	= 0.015
N × L	7.0	< 0.001	P × L	9.7	< 0.001
C × L	11.4	< 0.001	C × L	2.2	= 0.078
N × C × L	0.6	= 0.639	P × C × L	7.0	< 0.001
PIC:POC ratio					
N	934.6	< 0.001	P	395.0	< 0.001
C	81.8	< 0.001	C	9.1	= 0.004
L	30.9	< 0.001	L	47.6	< 0.001
N × C	6.6	= 0.013	P × C	13.4	< 0.001
N × L	9.8	< 0.001	P × L	14.4	< 0.001
C × L	6.8	< 0.001	C × L	1.5	= 0.202
N × C × L	0.7	= 0.567	P × C × L	4.7	= 0.002

N represents dissolved inorganic nitrogen (DIN, μmol l^{-1}); P represents dissolved inorganic phosphate (DIP, μmol l^{-1}); C represents pCO_2 (μatm); L represents light intensity (μmol photons m^{-2} s^{-1}); POC and PIC quotas represent particulate organic and inorganic carbon contents per cell, respectively

s^{-1} ($P > 0.05$) (Fig. 2a, c; Table 2), and they were higher at 480 μmol photons m^{-2} s^{-1} than at 320 μmol photons m^{-2} s^{-1} ($P < 0.01$). At HC, POC quotas increased significantly up to 480 μmol photons m^{-2} s^{-1} ($P < 0.01$). At LN, POC quotas increased when light intensity increased from 80 to 320 μmol photons m^{-2} s^{-1} ($P < 0.01$) and significantly declined thereafter (Fig. 2b).

In HNHP or LN treatments, at all light intensities, POC quotas did not show significant differences between HC and LC treatments ($P > 0.05$) (Fig. 2a, b). At LP, at 80 μmol photons m^{-2} s^{-1}, POC quotas were significantly higher at LC than at HC ($P < 0.01$), while at 480 μmol photons m^{-2} s^{-1} POC quotas were lower at LC than at HC ($P < 0.01$) (Fig. 2c).

At both LC and HC, within the light range of 80–320 μmol photons m^{-2} s^{-1}, POC quotas were not significantly different between LN and HNHP, and between LP and HNHP ($P > 0.05$), while at 480 μmol photons m^{-2} s^{-1}, they were lower at LN than at HNHP treatments ($P < 0.05$) (Fig. 2a, b). At LC and 480 μmol photons m^{-2} s^{-1}, POC quotas were significantly higher at HNHP than at LP ($P < 0.05$) (Fig. 2a, c).

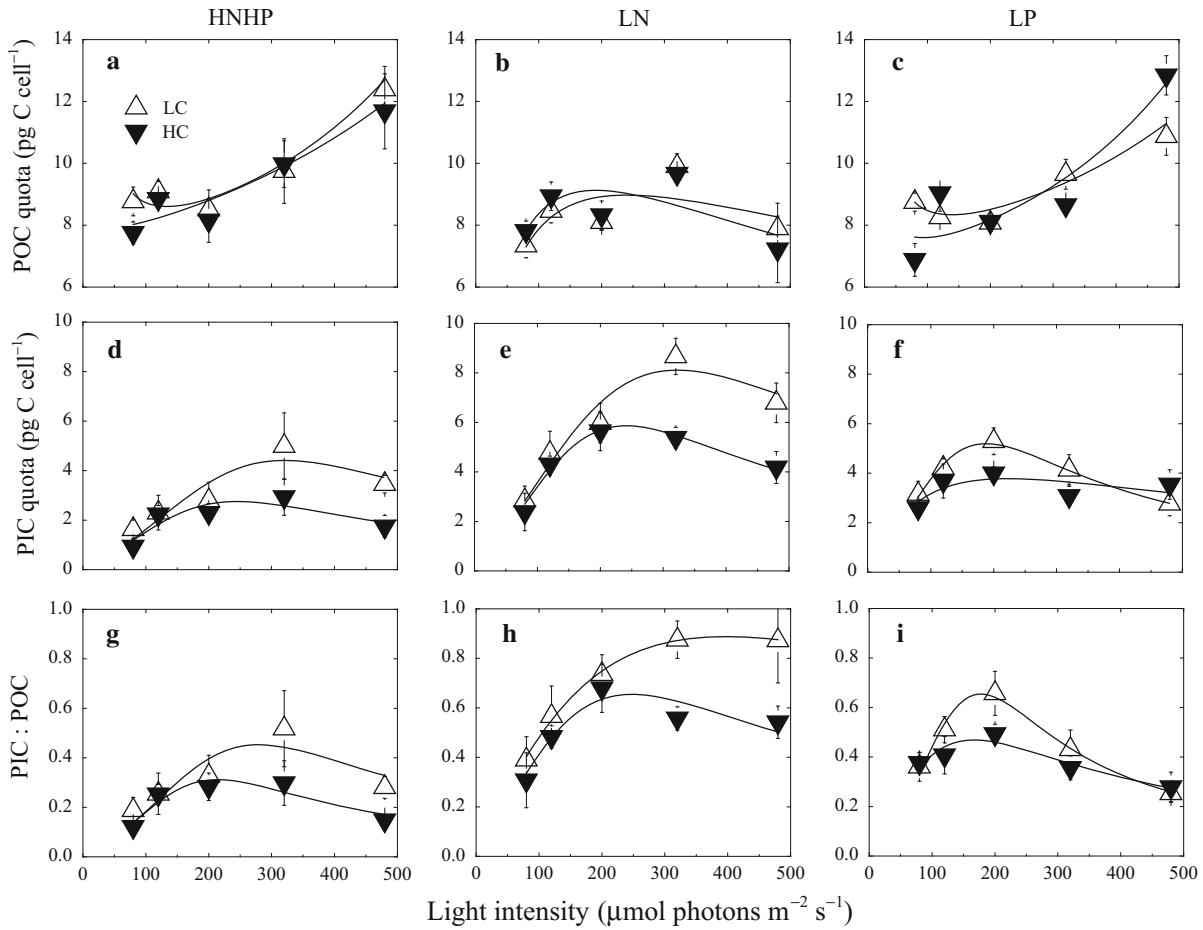

Fig. 2 At both LC (open symbols) and HC (solid symbols), POC quota of *E. huxleyi* as a function of light intensity under **a** HNHP, **b** LN, and **c** LP conditions. At both LC and HC, light response of PIC quota of *E. huxleyi* under **d** HNHP, **e** LN, and **f** LP conditions. At both LC and HC, light response of PIC:POC ratio of *E. huxleyi* under **g** HNHP, **h** LN, and **i** LP conditions. The lines in each panel were fitted using the model provided by Eilers and Peeters (1988). The values represent the mean ± standard deviation for four replicates

PIC quotas

In HNHP or LN treatments, PIC quotas increased significantly when light intensity increased from 80 to 320 µmol photons m^{-2} s^{-1} ($P < 0.05$) (Fig. 2d, e, Tables 2, S4), and declined thereafter (both $P > 0.1$ at LC and HC). At LP treatments and LC, PIC quotas increased significantly until 200 µmol photons m^{-2} s^{-1} ($P < 0.05$) (Fig. 2f), and declined with further increases in light intensity ($P < 0.05$) (Fig. 2f). At LP and HC, PIC quotas did not show significant differences at all light intensities ($P > 0.05$).

At HNHP or LN conditions, at 320 and 480 µmol photons m^{-2} s^{-1}, PIC quotas were larger at LC than at HC ($P < 0.05$) (Fig. 2d, e). At LP, at all light intensities, PIC quotas showed no significant differences between LC and HC treatments ($P > 0.05$) (Fig. 2f). Effects of CO_2 treatment on PIC quota were only significant at the optimum light intensity.

At both LC and HC, at all light intensities, PIC quotas were larger at LN than in HNHP treatments ($P > 0.05$ at 80 µmol photons m^{-2} s^{-1}; all $P < 0.05$ at 120–480 µmol photons m^{-2} s^{-1}) (Fig. 2d, e). At LC and HC, at 80–200 µmol photons m^{-2} s^{-1}, PIC quotas were significantly larger at LP than at HNHP ($P < 0.05$). At LC and 480 µmol photons m^{-2} s^{-1}, PIC quotas were significantly lower at LP than at HNHP ($P < 0.05$) (Fig. 2d, f).

PIC:POC ratio

At LC, in comparison to 80 µmol photons m^{-2} s^{-1}, PIC:POC ratio were significantly larger at 320 µmol photons m^{-2} s^{-1} under HNHP treatment, and at 200 µmol photons m^{-2} s^{-1} under LP treatment (both $P < 0.05$) (Fig. 2g, i, Tables 2, S4), while at HC, they were not significantly different between light treatments ($P > 0.05$). At LN, PIC:POC ratio increased significantly when light intensity increased from 80 to 200 µmol photons m^{-2} s^{-1} ($P < 0.01$) and did not show significant differences at 200–480 µmol photons m^{-2} s^{-1} ($P > 0.1$) (Fig. 2h).

PIC:POC ratios were not significantly different between LC and HC treatments regardless of the light treatments under HNHP or LP (all $P > 0.05$) (Fig. 2g, i). However, they were larger in LC than in HC treatments (both $P < 0.05$) at LN and 320 and 480 µmol photons m^{-2} s^{-1} (Fig. 2h).

At both LC and HC, at 80–480 µmol photons m^{-2} s^{-1}, PIC:POC ratios were larger at LN than at HNHP ($P > 0.05$ at 80 µmol photons m^{-2} s^{-1}; $P < 0.05$ at 120–480 µmol photons m^{-2} s^{-1}) (Fig. 2g, h), and low nitrate concentration was the most important factor regulating PIC:POC ratio. At both LC and HC, at 80–200 µmol photons m^{-2} s^{-1}, PIC:POC ratios were larger at LP than at HNHP (all $P < 0.05$) (Fig. 2g, i), while at 320 and 480 µmol photons m^{-2} s^{-1}, they were not significantly different between LP and HNHP treatments (both $P > 0.05$) (Fig. 2g, i).

Apparent light use efficiency and maximum value of growth, POC and PIC production rates

At each nutrient treatment, *alpha* values of fitted curves of growth, POC and PIC production rates were not significantly different between LC and HC, with the exception of *alpha* of PIC production rate at LP ($P < 0.05$) (Fig. 3; Table S5). At both LC and HC, *alpha* values of fitted curves of growth and POC production rates did not show significant differences between HNHP, LN, and LP treatments, with the exception of *alpha* of POC production rate between HNHP–LC and LP–HC treatments ($P < 0.05$) (Fig. 3c). At LN under both LC and HC, and at LP under LC, *alpha* values of PIC production rates were larger than those of POC production rates, which were larger than those of growth rates (all $P < 0.01$) (Fig. 3a, c, e).

At HNHP, LN, or LP treatment, maximum growth rates were significantly larger at LC than at HC (all $P < 0.05$) (Fig. 3b). At both LC and HC, maximum growth rates were larger at HNHP than at LN (both $P < 0.05$), and they were similar between HNHP and LP (both $P > 0.05$) (Fig. 3b).

At each nutrient treatment, maximum POC production rates were slightly larger at LC than at HC (all $P > 0.05$) (Fig. 3d). At LC, maximum POC production rate was lower at LN than at HNHP and LP treatments ($P < 0.05$ between LN and HNHP; $P > 0.05$ between LN and LP). At HC, they did not show significant differences between HNHP, LN, and LP treatments ($P > 0.05$) (Fig. 3d).

At HNHP, LN, or LP treatment, maximum PIC production rates were significantly larger at LC than at HC (all $P < 0.05$) (Fig. 3f). At both LC and HC, maximum PIC production rates were larger at LN than at HNHP or LP treatment ($P < 0.05$) (Fig. 3f). Overall, low nitrate concentrations significantly affected maximum growth rate, POC and PIC quotas.

Discussion

CO_2 modulated responses of growth and POC quota to availability of nitrate and light

Effects of rising CO_2 on light responses of growth rate, POC and PIC quotas or production rates of coccolithophores were reported by a number of studies (Feng et al., 2008; Zhang et al., 2015; Jin et al., 2017; Gafar et al., 2018). However, few studies investigate modulation of CO_2 on light response curves of physiological rates of coccolithophores at different nutrient concentrations. By fitting the light response curves, our data showed that low nitrate concentration and high CO_2 level synergistically reduced maximum growth and POC production rates of *E. huxleyi*. Furthermore, POC quotas and production rates were more affected by low nitrate concentration and light intensity than by CO_2 levels (Figs. 2, 3, S4).

While 1 µmol l^{-1} dissolved inorganic nitrogen (DIN) was measured at the end of incubation at LN treatments (Table S2), limiting DIN levels during the incubation could play more inhibitive roles for the limited growth and POC quota (Harrison & Li, 2008). Unfortunately, we did not measure the cell abundance every day, and cells sampled were expected to be in

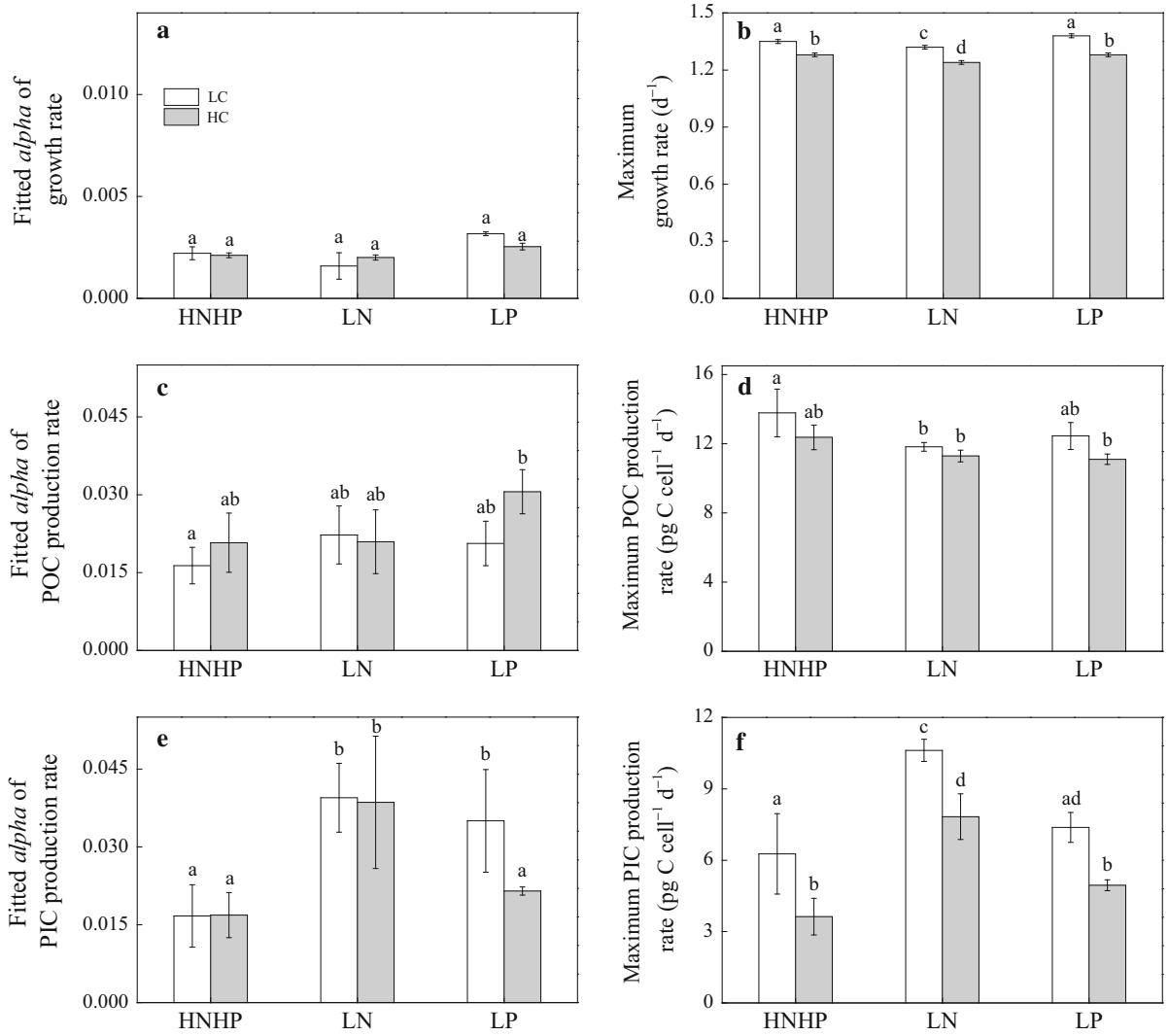

Fig. 3 At both LC (open symbols) and HC (solid symbols), fitted *alpha* (left) and maximum values (right) of growth rate (**a**, **b**), POC production rate (**c**, **d**), and PIC production rate (**e**, **f**) under HNHP, LN, and LP conditions. *alpha* was the slope of fitted lines for growth, POC and PIC production rates. Different letters showed statistical differences based on the Tukey post hoc test. The values represent the mean ± standard deviation for four replicates

exponential phase on the basis of final cell concentrations (Table S3) (Langer et al., 2013). Based on measured particulate organic nitrogen (PON) quota and cell concentration in this study (Fig. S3, Table S3), PON concentrations at the end of incubations were estimated to be 7.8–9.3 μmol l^{-1} at different nutrient treatments. These data were closely correlated with molar drawdown of DIN during the incubation at LN treatments (Table S2). Furthermore, POC quotas and PON quotas were lower in the nutrient-limited cells than in the control under all treatments, suggesting that POC and PON production rates were not caused by a methodological artifact in the batch cultures in this study (Langer et al., 2013).

Another possible reason for low growth and POC quota at LN treatment may be that synthesis of amino acids, activity of nitrate reductase, and nitrogen metabolism may be reduced in *E. huxleyi* (Bruhn et al., 2010; Rouco et al., 2013; Rokitta et al., 2014). This could indicate lower overall biosynthetic activity, and thus decreases in the growth and POC quota (Figs. 1, 2). Reduced availability of nitrate limited the

synthesis of pigments, which may reduce energy availability absorbed by light-absorbing pigments and thus reduce growth and carbon fixation. Synergistic effects of LN and HC treatments on growth and POC production rates indicate that these treatments may inhibit cellular metabolic activity simultaneously (Figs. 1, 3) (Sciandra et al., 2003). In fact, intracellular $[H^+]$ has been reported to be higher in HC-grown than in LC-grown *E. huxleyi* cells (Suffrian et al., 2011). To transport extra H^+ out of cells, *E. huxleyi* at HC needs more transporters and energy, but LN is unlikely to provide necessary nitrogen supplies for the synthesis of these transporters and energy supply (Fig. S3). Therefore, reduced nitrate availability exacerbated the negative effects of OA on growth of *E. huxleyi*, supporting previous findings (Bruhn et al., 2010).

CO_2 and light modulated responses of growth and POC quota to phosphate concentration

E. huxleyi possesses an exceptional phosphorus acquisition capacity, which could allow it to dominate in phosphate-limiting environments (Dyhrman & Palenik, 2003). In this study, low light intensity not only limited cell growth but could also limit phosphate uptake rates (Nalewajko & Lee, 1983). In this case, compared to the HNHP treatment, growth rates of *E. huxleyi* were more likely to be limited by low phosphate concentration at low light intensity (Fig. 1a, c). High light intensity provided energy for cells to take up P, and cells at LP treatments need to consume more energy to up-regulate P uptake (Nalewajko & Lee, 1983) which may lead to decreased high-light inhibition of growth rate at LP than at HNHP treatments under LC. Furthermore, growth rate of *E. huxleyi* was saturated at 0.5 µM DIP and above (Fig. 4). This demonstrated that *E. huxleyi* possesses a high affinity for DIP and could take up PO_4^{3-} efficiently. In addition, *E. huxleyi* could store phosphorus within cells or scavenge bioavailable phosphate from membrane structure of cells at P-limitation (Rokitta et al., 2016; Shemi et al., 2016). Consequently, high energy consumption, efficient uptake, storage capacity, or re-allocation of phosphorus in *E. huxleyi* may account for the insignificant differences observed in growth rates between LP and HNHP treatments under LC and high light intensity (Fig. 1a, c).

Rising CO_2 increased cell volume under the highest light intensity (Table S3). Large cell volume can directly lead to lower growth rates or reduce nutrient uptake by cells, thereby limiting growth (Finkel, 2001). Another possible reason for low tolerance to high light intensity in growth rate at LP and HC treatments might be a combined effect of LP and HC on the carbon concentrating mechanism (CCM) of *E. huxleyi*. LP and/or HC is hypothesized to down-regulate the activity of CCMs in the green alga *Chlorella emersonii* and in other typical phytoplankton species (Chen & Gao, 2003; Rost & Riebesell, 2004; Beardall et al., 2005). When grown at HC, LP may minimize the activity of CCM of *E. huxleyi*, which could lead to less energetic cost for sustaining the operation of CCM. The energy saved in the HC- and LP-grown cells might have exacerbated photoinhibition (Borchard et al., 2011). Thus, large cell volume and less energy consumption at LP and HC treatments may lead to increased high-light inhibition of growth rates of *E. huxleyi* (Fig. 1).

Low nutrient concentrations facilitated calcification rate

In this study, we showed that decreased availability of the nutrients, especially of nitrate, facilitated PIC quotas and production rates (Fig. 2), being consistent

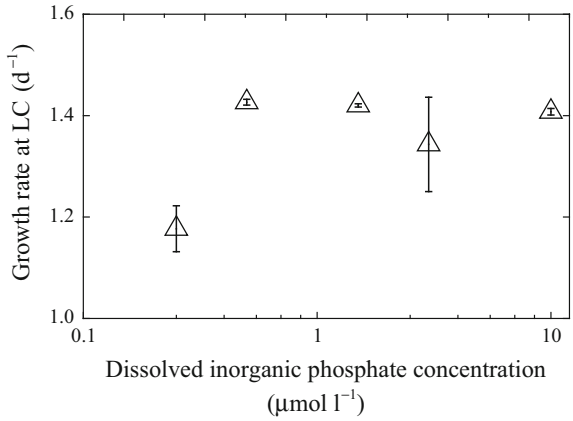

Fig. 4 At LC, growth rate of *E. huxleyi* as a function of dissolved inorganic phosphate (DIP) concentration. DIN concentration was 100 µmol l^{-1} in all culture media, and initial DIP concentrations were set up to 0.25 µmol l^{-1}, 0.5 µmol l^{-1}, 1.5 µmol l^{-1}, 3 µmol l^{-1}, and 10 µmol l^{-1} in the culture media. All samples were incubated at 200 µmol photons m^{-2} s^{-1} and at 410 µatm pCO_2 for 4 days, and the values represent the mean ± standard deviation for three replicates

with results reported by Nimer & Merrett (1993). Due to lower POC and PON quotas and lower growth rate, we could expect that at LN, more energy was reallocated to synthesize particulate inorganic carbon (Figs. 1, 2, S3, S4). At LP, slightly larger PIC quota is likely due to larger cell volume in comparison with the HNHP treatment (Fig. 2). Reduced availability of phosphate may prevent cell division, indirectly leading to higher PIC quota (Müller et al., 2008). It should be mentioned that cells on the sampling days were more likely in the late exponential phase, and to be limited by the nutrients at LN and LP treatments. On the other hand, larger PIC:POC ratios have the potential to accelerate sinking rate of *E. huxleyi* cells, facilitating the export of carbon into deeper waters (Hoffmann et al., 2015).

To provide organic carbon fixed by photosynthesis to support growth and other metabolic processes, cells need to maintain larger light use efficiency (*alpha*) for POC production rates even at low light intensities (Fig. 3c). To calcify, *E. huxleyi* cells need to take up HCO_3^- and Ca^{2+} from the medium, which consumes energy. Besides that, they also need to extrude H^+ generated during calcification, which may also require extra energy (Paasche 2002). Thus, calcification is an energy-consuming process. To maintain high calcification rates at low nutrient concentrations, cells possessing high efficiencies for light can obtain more energy to take up HCO_3^- and Ca^{2+}, and extrude H^+ (Fig. 3e). Via photosynthesis, algae convert light energy to chemical energy (ATP and NADPH) which can be used for carboxylation. In coccolithophores, such chemical energy is also used for calcification. Therefore, we suggest that energy may first be allocated to photosynthetic carbon fixation, and then to calcification.

Using a chemostat culture, Müller et al. (2017) reported that DIN or DIP limitation decreased the POC and PIC production rates (in pg C $cell^{-1}$ d^{-1}) by 50%, and rising pCO_2 levels did not affect POC production rates. However, when normalized to cell volume, nutrient limitation did not affect POC and PIC production rates [in pg C (cell volume)$^{-1}$ d^{-1}], and rising pCO_2 levels reduced POC and PIC production rates. In our study, decreased DIN or DIP concentrations reduced the normalized POC production rates [in pg C (cell volume)$^{-1}$ d^{-1}], and increased the normalized PIC production rates at both LC and HC (Figs. S5, S6). Differential results between this study and that of Müller et al. (2017) may result from different experimental setups or light exposures used. Growth was limited by N or P when cells were cultured in a 24-h light condition without darkness, and cell growth was in the stationary phase when POC and PIC samples were taken in the study of Müller et al. (2017). In comparison, we took POC and PIC samples in the exponential growth phase, and LN or LP also appeared to limit growth of *E. huxleyi*. However, different light sources or daytime exposure doses of different light wavelengths may bring out different indoor experimental results (Xing et al., 2015).

Nutrient availability, CO_2 level, and light intensity significantly interacted to affect growth rate, POC and PIC quotas (Table 2). Obviously, the question of how growth, carbon fixation, and calcification rates of *E. huxleyi* would respond to ocean global changes needs to be examined under multiple stressors (Boyd et al., 2018) and under natural environmental variations (Feng et al., 2008, 2017). While temperature was not included in this work, it is most likely that rising temperature can modulate the effects we showed here, which is worth investigating in future. Although HC treatment reduced calcification rates of *E. huxleyi*, low nutrient concentrations showed dominant positive effects on PIC quota or calcification rate (Fig. 2d–f), and increased solar exposure can partly counteract the negative effects of OA (Jin et al., 2017). This suggests that controls on calcification of *E. huxleyi* might be more complex than expected. Effects of CO_2 and light intensity on growth, POC and PIC quotas of *E. huxleyi* were strongly modulated by nutrient concentrations, which showed the importance of nutrient concentrations on controlling physiological processes of coccolithophores. Obviously, complex interactive effects of multiple environmental drivers on primary producers are likely to differ from that of single or two factorial combinations, so it is important for us to examine effects of multiple stressors to comprehend how ecological and biogeochemical functions of key phytoplankton groups may respond to ocean global changes.

Conclusions

This study showed that rising CO_2 concentrations relevant to ocean acidification modulated the

physiological responses of *E. huxleyi* to nutrient availability and changes in light intensity. With increasing atmospheric CO_2 concentration and progressive ocean warming and acidification, the oceanic upper mixed layer will shoal, therefore exposing coccolithophores within this layer to higher levels of daily integrated sunlight and reduced levels of nutrients due to less upward advective transport. This work showed that elevated CO_2 (900 μatm) exacerbated photo-inhibition of the growth rate under reduced availability of phosphate under high light levels; and low nitrate and high CO_2 levels synergistically reduced the growth rate. These results imply that growth of *E. huxleyi* may decrease in pelagic waters with enhanced stratification associated with ocean warming and acidification, though higher ratios of PIC to POC at reduced nutrient concentrations may counteract to some extent the negative effects of OA on calcification.

Acknowledgements This study was supported by the National Natural Science Foundation (41720104005, 41721005, 41806129), and Joint project of National Natural Science Foundation of China and Shandong province (No. U1606404), China Postdoctoral Science Foundation (2017M612129), and the outstanding postdoctoral program of State Key Laboratory of Marine Environmental Science (Xiamen University). FF and DH's visits to Xiamen were supported by MEL's visiting scientist program, and their contributions were supported by U.S. National Science Foundation grants OCE 1538525 and 1638804.

References

Bach, L. T., U. Riebesell & K. G. Schulz, 2011. Distinguishing between the effects of ocean acidification and ocean carbonation in the coccolithophore *Emiliania huxleyi*. Limnology and Oceanography 56: 2040–2050.

Bach, L. T., U. Riebesell, M. A. Gutowska, L. Federwisch & K. G. Schulz, 2015. A unifying concept of coccolithophore sensitivity to changing carbonate chemistry embedded in an ecological framework. Progress in Oceanography 135: 125–138.

Beardall, J., S. Roberts & J. A. Raven, 2005. Regulation of inorganic carbon acquisition by phosphorus limitation in the green alga *Chlorella emersonii*. Canadian Journal of Botany 83: 859–864.

Behrenfeld, M., R. O'Malley, D. Siegel, C. McClain, J. Sarmiento, G. Feldman, A. Milligan, P. Falkowski, R. Letelier & E. Boss, 2006. Climate-driven trends in contemporary ocean productivity. Nature 444: 752–755.

Borchard, C., A. V. Borges, N. Händel & A. Engel, 2011. Biogeochemical response of *Emiliania huxleyi* (PML B92/11) to elevated CO_2 and temperature under phosphorous limitation: a chemostat study. Journal of Experimental Marine Biology and Ecology 410: 61–71.

Boyd, P. W., S. T. Lennartz, D. M. Glover & S. C. Doney, 2015. Biological ramifications of climate-change-mediated oceanic multi-stressors. Nature Climate Change 5: 71–79.

Boyd, P. W., P. W. Dillingham, C. M. McGraw, E. A. Armstrong, C. E. Cornwall, F. F. Feng, C. L. Hurd, M. Gault-Ringold, M. Y. Roleda, E. Timmins-Schiffman & B. L. Nunn, 2016. Physiological responses of a Southern Ocean diatom to complex future ocean conditions. Nature Climate Change 6: 207–213.

Boyd, P. W., S. Collins, S. Dupont, K. Fabricius, J. P. Gattuso, J. Havenhand, D. A. Hutchins, U. Riebesell, M. S. Rintoul, M. Vichi, H. Biswas, A. Ciotti, K. Gao, M. Gehlen, C. L. Hurd, H. Kurihara, C. M. McGraw, J. M. Navarro, G. E. Nilsson, U. Passow & H. O. Pörtner, 2018. Experimental strategies to assess the biological ramifications of multiple drivers of global ocean change—a review. Global Change Biology 24: 1–23.

Brennan, G. & S. Colllins, 2015. Growth responses of a green alga to multiple environmental drivers. Nature Climate Change 5: 892–897.

Bruhn, A., J. LaRoche & K. Richardson, 2010. *Emiliania huxleyi* (Prymnesiophyceae): nitrogen-metabolism genes and their expression in response to external nitrogen sources. Journal of Phycology 46: 266–277.

Caldeira, K. & M. E. Wickett, 2003. Oceanography: anthropogenic carbon and ocean pH. Nature 425: 365.

Chen, X. & K. Gao, 2003. Effect of CO_2 concentrations on the activity of photosynthetic CO_2 fixation and extracelluar carbonic anhydrase in the marine diatom *Skeletonema costatum*. Chinese Science Bulletin 48: 2616–2620.

Chou, W. C., D. D. Sheu, C. A. Chen, S. L. Wang & C. M. Tseng, 2005. Seasonal variability of carbon chemistry at the SEATS time-series site, Northern South China Sea betweeen 2002 and 2003. Terrestrial Atmospheric and Oceanic Sciences 16: 445–465.

Cloern, J. E., 1999. The relative importance of light and nutrient limitation of phytoplankton growth: a simple index of coastal ecosystem sensitivity to nutrient enrichment. Aquatic Ecology 33: 3–16.

Dickson, A. G., 1993. pH buffers for sea water media based on the total hydrogen ion concentration scale. Deep Sea Research 40: 107–118.

Dickson, A. G., J. D. Afghan & G. C. Anderson, 2003. Reference materials for oceanic CO_2 analysis: a method for the certification of total alkalinity. Marine Chemistry 80: 185–197.

Dyhrman, S. T. & B. Palenik, 2003. Characterization of ectoenzyme activity and phosphate-regulated proteins in the coccolithophorid *Emiliania huxleyi*. Journal of Plankton Research 25: 1215–1225.

Eilers, P. & J. Peeters, 1988. A model for the relationship between light intensity and the rate of photosynthesis in phytoplankton. Ecological Modelling 42: 199–215.

Feng, Y. Y., M. E. Warner, Y. H. Zhang, J. Sun, F. X. Fu, J. M. Rose & D. A. Hutchins, 2008. Interactive effects of increased pCO_2, temperature and irradiance on the marine coccolithophore *Emiliania huxleyi* (Prymnesiophyceae). European Journal of Phycology 43: 87–98.

Feng, Y. Y., M. Y. Roleda, E. Armstrong, P. W. Boyd & C. L. Hurd, 2017. Environmental controls on the growth, photosynthetic and calcification rates of a Southern Hemisphere strain of the coccolithophore *Emiliania huxleyi*. Limnology and Oceanography 62: 519–540.

Finkel, Z. V., 2001. Light absorption and size scaling of light-limited metabolism in marine diatoms. Limnology and Oceanography 46: 86–94.

Gafar, N. A., B. D. Eyre & K. G. Schulz, 2018. A conceptual model for projecting coccolithophorid growth, calcification and photosynthetic carbon fixation rates in response to global ocean change. Frontiers in Marine Science 4: 433.

Gao, K. S., J. T. Xu, G. Gao, Y. H. Li, D. A. Hutchins, B. Q. Huang, L. Wang, Y. Zheng, P. Jin, X. N. Cai, D. P. Häder, W. Li, K. Xu, N. N. Liu & U. Riebesell, 2012a. Rising CO_2 and increased light exposure synergistically reduce marine primary productivity. Nature Climate Change 2: 519–523.

Gao, K., E. W. Helbling, D. P. Häder & D. A. Hutchins, 2012b. Responses of marine primary producers to interactions between ocean acidification, solar radiation, and warming. Marine Ecology Progress Series 470: 167–189.

Geider, R. J., H. L. MacIntyre & T. M. Kana, 1997. A dynamic model of phytoplankton growth and acclimation: responses of the balanced growth rate and chlorophyll *a*: carbon ratio to light, nutrient-limitation and temperature. Marine Ecology Progress Series 148: 187–200.

Hansen, H. P. & F. Koroleff, 1999. Determination of nutrients. In Grasshoff, K., K. Kremling & M. Ehrhardt (eds), Methods of Seawater Analysis. Wiley, New Yrok: 159–228.

Harrison, W. G. & W. K. W. Li, 2008. Phytoplankton growth and regulation in the Labrador Sea: light and nutrient limitation. Journal of Northwest Atlantic Fishery Science 39: 71–82.

Hoffmann, R., C. Kirchlechner, G. Langer, A. S. Wochnik, E. Griesshaber, W. W. Schmah & C. Scheu, 2015. Insight into *Emiliania huxleyi* coccospheres by focused ion beam sectioning. Biogeosciences 12: 825–834.

Hutchins, D. A. & F. X. Fu, 2017. Microorganisms and ocean global change. Nature Microbiology 2: 17058.

Jin, P., J. Ding, T. Xing, U. Riebesell & K. Gao, 2017. High levels of solar radiation offset impacts of ocean acidification on calcifying and non-calcifying strains of *Emiliania huxleyi*. Marine Ecology Progress Series 568: 47–58.

Kim, H. S., S. J. Hwang, J. K. Shin, K. G. An & C. G. Yoon, 2007. Effects of limiting nutrients and N: P ratios on the phytoplankton growth in a shallow hypertrophic reservoir. Hydrobiologia 581: 255–267.

Kottmeier, D. M., S. D. Rokitta & B. Rost, 2016. Acidification, not carbonation, is the major regulator of carbon fluxes in the coccolithophore *Emiliania huxleyi*. New Phytologist 211: 126–137.

Langer, G., G. Nehrke, I. Probert, J. Ly & P. Ziveri, 2009. Strain-specific responses of *Emiliania huxleyi* to changing seawater carbonate chemistry. Biogeosciences 6: 2637–2646.

Langer, G., K. Oetjen & T. Brenneis, 2013. Coccolithophores do not increase particulate carbon production under nutrient limitation: a case study using *Emiliania huxleyi* (PML92/11). Journal of Experimental Marine Biology and Ecology 443: 155–161.

Larsen, A., G. A. F. Flaten, R. Sandaa, T. Castberg, R. Thyrhaug, S. R. Erga, S. Jacquet & G. Bratbak, 2004. Spring phytoplankton bloom dynamics in Norwegian coastal waters: microbial community succession and diversity. Limnology and Oceanography 49: 180–190.

Leonardos, N. & R. J. Geider, 2005. Eleveted atmospheric carbon dioxide increases organic carbon fixation by *Emiliania huxleyi* (Haptophyta), under nutrient-limited high-light conditions. Journal of Phycology 41: 1196–1203.

Matthiessen, B., S. L. Eggers & S. A. Krug, 2012. High nitrate to phosphorus regime attenuates negative effects of rising pCO_2 on total population carbon accumulation. Biogeosciences 9: 1195–1203.

McKew, B. A., P. Davey, S. J. Finch, J. Hopkins, S. C. Lefebvre, M. V. Metodiev, K. Oxborough, C. A. Raines, T. Lawso & R. J. Geider, 2013. The trade-off between the light-harvesting and photoprotective functions of fucoxanthin-chlorophyll proteins dominates light acclimation in *Emiliania huxleyi* (clone CCMP 1516). New Phytologist 200: 74–85.

McKew, B. A., G. Metodieva, C. A. Raines, M. V. Metodier & R. J. Geider, 2015. Acclimation of *Emiliania huxleyi* (1516) to nutrient limitation involves precise modification of the proteome to scavenge alternative sources of N and P. Environmental Microbiology 17: 4050–4062.

Meyer, J. & U. Riebesell, 2015. Reviews and syntheses: responses of coccolithophores to ocean acidification: a meta-analysis. Biogeosciences 12: 1671–1682.

Müller, M. N., A. N. Antia & J. LaRoche, 2008. Influence of cell cycle phase on calcification in the coccolithophore *Emiliania huxleyi*. Limnology and Oceanography 53: 506–512.

Müller, M. N., L. Beaufort, O. Bernard, M. L. Pedrotti, A. Talec & A. Sciandra, 2012. Influence of CO_2 and nitrogen limitation on the coccolith volume of *Emiliania huxleyi* (Haptophyta). Biogeosciences 9: 4155–4167.

Müller, M. N., T. W. Trull & G. M. Hallegraeff, 2017. Independence of nutrient limitation and carbon dioxide impacts on the Southern Ocean coccolithophore *Emiliania huxleyi*. ISME Journal 11: 1777–1787.

Nalewajko, C. & K. Lee, 1983. Light stimulation of phosphate uptake in marine phytoplankton. Marine Biology 74: 9–15.

Nimer, N. A. & M. J. Merrett, 1993. Calcification rate in *Emiliania huxleyi* Lohmann in response to light, nitrate and availability of inorganic carbon. New Phytologist 123: 673–677.

Omar, A. M., A. Olsen, T. Johannessen, M. Hoppema, H. Thomas & A. V. Borges, 2010. Spatiotemporal variations of fCO_2 in the North Sea. Ocean Science 6: 77–89.

Paasche, E., 2002. A review of the coccolithophorid *Emiliania huxleyi* (Prymnesiophyceae), with particular reference to growth, coccolith formation, and calcification-photosynthesis interactions. Phycologia 40: 503–529.

Pierrot, D., E. Lewis & D. W. R. Wallace, 2006. MS Excel Program Developed for CO_2 System Calculations, ORNL/CDIAC-105. Department of Energy, Carbon Dioxide Information Analysis Centre, Oak Ridge National Laboratory, Oak Ridge.

Richier, S., S. Fiorini, M. E. Kerros, P. Von Dassow & J. P. Gattuso, 2011. Response of the calcifying

coccolithophore *Emiliania huxleyi* to low pH/high pCO_2: from physiology to molecular level. Marine Biology 158: 551–560.

Riegman, R., W. Stolte, A. A. M. Noordeloos & D. Slezak, 2000. Nutrient uptake and alkaline phosphatase (EC3:1:3:1) activity of *Emiliania huxleyi* (Prymnesiophyceae) during growth under N and P limitation in continuous cultures. Journal of Phycology 36: 87–96.

Rokitta, S. D., P. von Dassow, B. Rost & U. John, 2014. *Emiliania huxleyi* endures N-limitation with an efficient metabolic budgeting and effective ATP synthesis. BMC Genomics 15: 1051–1064.

Rokitta, S. D., P. von Dassow, B. Rost & U. John, 2016. P- and N-depletion trigger similar cellular responses to promote senescence in eukaryotic phytoplankton. Frontiers in Marine Science 3: 109.

Rost, B. & U. Riebesell, 2004. Coccolithophores and the biological pump: responses to environmental changes. In Thierstein, H. R. & J. Young (eds), Coccolithophores—From Molecular Biology to Global Impact. Springer, Berlin: 99–125.

Rouco, M., O. Branson, M. Lebrato & M. D. Iglesias-Rodríguez, 2013. The effect of nitrate and phosphate availability on *Emiliania huxleyi* (NZEH) physiology under different CO_2 scenarios. Frontiers in Microbiology 4: 155.

Roy, R. N., L. N. Roy, K. M. Vogel, C. Porter-Moore, T. Pearson, C. E. Good, F. J. Millero & D. C. Campbell, 1993. Thermodynamics of the dissociation of boric acid in seawater at S 5 35 from 0 degrees C to 55 degrees C. Marine Chemistry 44: 243–248.

Sciandra, A., J. Harlay, D. Lefévre, R. Lemée, P. Rimmelin, M. Denis & J. P. Gattuso, 2003. Response of coccolithophorid *Emiliania huxleyi* to elevated partial pressure of CO_2 under nitrogen limitation. Marine Ecology Progress Series 261: 111–122.

Sett, S., L. T. Bach, K. G. Schulz, S. Koch-Klavsen, M. Lebrato & U. Riebesell, 2014. Temperature modulates coccolithophorid sensitivity of growth, photosynthesis and calcification to increasing seawater pCO_2. PLOS ONE 9: e88308.

Shemi, A., D. Schatz, H. F. Fredricks, B. A. S. Van Mooy, Z. Porat & A. Vardi, 2016. Phosphorus starvation induces membrane remodeling and recycling in *Emiliania huxleyi*. New Phytologist 211: 886–898.

Steinacher, M., F. Joos, T. L. Frölicher, L. Bopp, P. Cadule, V. Cocco, S. C. Doney, M. Gehlen, K. Lindsay, J. K. Moore, B. Schneider & J. Segschneider, 2010. Projected 21st century decrease in marine productivity: a multi-model analysis. Biogeosciences 7: 979–1005.

Suffrian, K., K. G. Schulz, M. Gutowska, U. Riebesell & M. Bleich, 2011. Cellular pH measurements in *Emiliania huxleyi* reveal pronounced membrane proton permeability. New Phytologist 190: 595–608.

Sunda, W. G., N. M. Price & F. M. M. Morel, 2005. Trace metal ion buffers and their use in culture studies. In Andersen, R. A. (ed.), Algal Culturing Techniques. Elsevier Academic Press, London: 53–59.

Tong, S. Y., D. A. Hutchins, F. X. Fu & K. S. Gao, 2016. Effects of varying growth irradiance and nitrogen sources on calcification and physiological performance of the coccolithophore *Gephyrocapsa oceanica* grown under nitrogen limitation. Limnology and Oceanography 61: 2234–2242.

Wang, G., S. P. Xie, R. X. Huang & C. Chen, 2015. Robust warming pattern of global subtropical oceans and its mechanism. Journal of Climate 28: 8574–8584.

Xing, T., K. Gao & J. Beardall, 2015. Response of growth and photosynthesis of *Emiliania huxleyi* to visible and UV irradiances under different light regimes. Photochemistry and Photobiology 91: 343–349.

Zhang, Y., L. T. Bach, K. G. Schulz & U. Riebesell, 2015. The modulating effect of light intensity on the response of the coccolithophore *Gephyrocapsa oceanica* to ocean acidification. Limnology and Oceanography 60: 2145–2157.

Zhang, Y., L. T. Bach, K. T. Lohbeck, K. G. Schulz, L. Listmann, R. Klapper & U. Riebesell, 2018. Population-specific responses in physiological rates of Emilinia huxleyi to a broad CO_2 range. Biogeosciences 15: 3691–3701.